RESEARCH ARTICLE

National Science Review
5: 500–506, 2018
doi: 10.1093/nsr/nwy004
Advance access publication 9 January 2018

PHYSICS

Dimensional crossover of heat conduction in amorphous polyimide nanofibers

Lan Dong[1,2,3], Qing Xi[1,2,3], Dongsheng Chen[4,5], Jie Guo[1,2,3], Tsuneyoshi Nakayama[1,2,3,6], Yunyun Li[1,2,3], Ziqi Liang[4], Jun Zhou[1,2,3,*], Xiangfan Xu[1,2,3,*] and Baowen Li[7,*]

[1]Center for Phononics and Thermal Energy Science, School of Physics Science and Engineering, Tongji University, Shanghai 200092, China; [2]China-EU Joint Center for Nanophononics, School of Physics Science and Engineering, Tongji University, Shanghai 200092, China; [3]Shanghai Key Laboratory of Special Artificial Microstructure Materials and Technology, School of Physics Science and Engineering, Tongji University, Shanghai 200092, China; [4]Department of Materials Science, Fudan University, Shanghai 200433, China; [5]College of Mathematics and Physics, Shanghai University of Electric Power, Shanghai 200090, China; [6]Hokkaido University, Sapporo 060-0826, Japan and [7]Department of Mechanical Engineering, University of Colorado, Boulder, CO 80309-0427, USA

*Corresponding authors. E-mails: xuxiangfan@tongji.edu.cn; zhoujunzhou@tongji.edu.cn; Baowen.Li@Colorado.EDU

Received 21 August 2017; **Revised** 12 December 2017; **Accepted** 6 January 2018

ABSTRACT

The mechanism of thermal conductivity in amorphous polymers, especially polymer fibers, is unclear in comparison with that in inorganic materials. Here, we report the observation of a crossover of heat conduction behavior from three dimensions to quasi-one dimension in polyimide nanofibers at a given temperature. A theoretical model based on the random walk theory has been proposed to quantitatively describe the interplay between the inter-chain hopping and the intra-chain hopping in nanofibers. This model explains well the diameter dependence of thermal conductivity and also speculates on the upper limit of thermal conductivity of amorphous polymers in the quasi-1D limit.

Keywords: dimensional crossover, thermal conductivity, nanofiber

INTRODUCTION

Polymers are widely used materials due to their fascinating properties such as low mass density, chemical stability and high malleability, etc. [1]. Unfortunately, the relatively low thermal conductivity of polymer, which is in the range of ∼0.1 Wm^{-1} K^{-1} to ∼0.3 Wm^{-1} K^{-1} [2–4], limits its application in thermal management. The low thermal conductivity of polymer is considered to be one of the major reasons for the thermal failure in electronic devices [5,6]. Therefore, thermally conductive polymers are highly demanded for heat dissipation in microelectronic and civil applications.

In contrast to common wisdom, polymer nanofibers hold surprisingly high thermal conductivity; some of them are even comparable to that in some metals or even silicon. Choy and his co-workers carried out the pioneering theory and experiments to demonstrate that the alignment of molecular chains could enhance the thermal conductivity along the alignment direction [7–9]. The increase of the thermal conductivity is attributed to the increase of the degree of crystallinity in subsequent experimental works [1,10–12]. Cai *et al.* also observed thermal conductivity enhancement in polyethylene nanowires fabricated by the improved nanoporous template wetting technique, due to the high chain orientation arising from crystallinity [13,14]. More recently, Singh *et al.* demonstrated that better molecular chain orientation could also improve the thermal conductivity when polymer fibers remain amorphous [4], which indicates that it is also of significance to study the intrinsic mechanism of thermal conductivity in amorphous polymer. All these pioneering works indicate that the thermal properties in polymers are highly related to their microscopic configurations, and thermal conductivity is limited by the molecular orientation and the inter-chain scatterings [15,16].

It has also been found that through molecular dynamics (MD) simulation that the chain conformation would strongly influence thermal conductivity [17,18]. However, very few theories have been proposed to quantitatively study the structure dependence of thermal conductivity in amorphous polymers because of their complex intrinsic structure. Alternatively, theories for amorphous inorganic materials such as heat transfer by diffusons [19,20], the minimum thermal conductivity model [21–23] and the phonon-assisted hopping model [24–26]

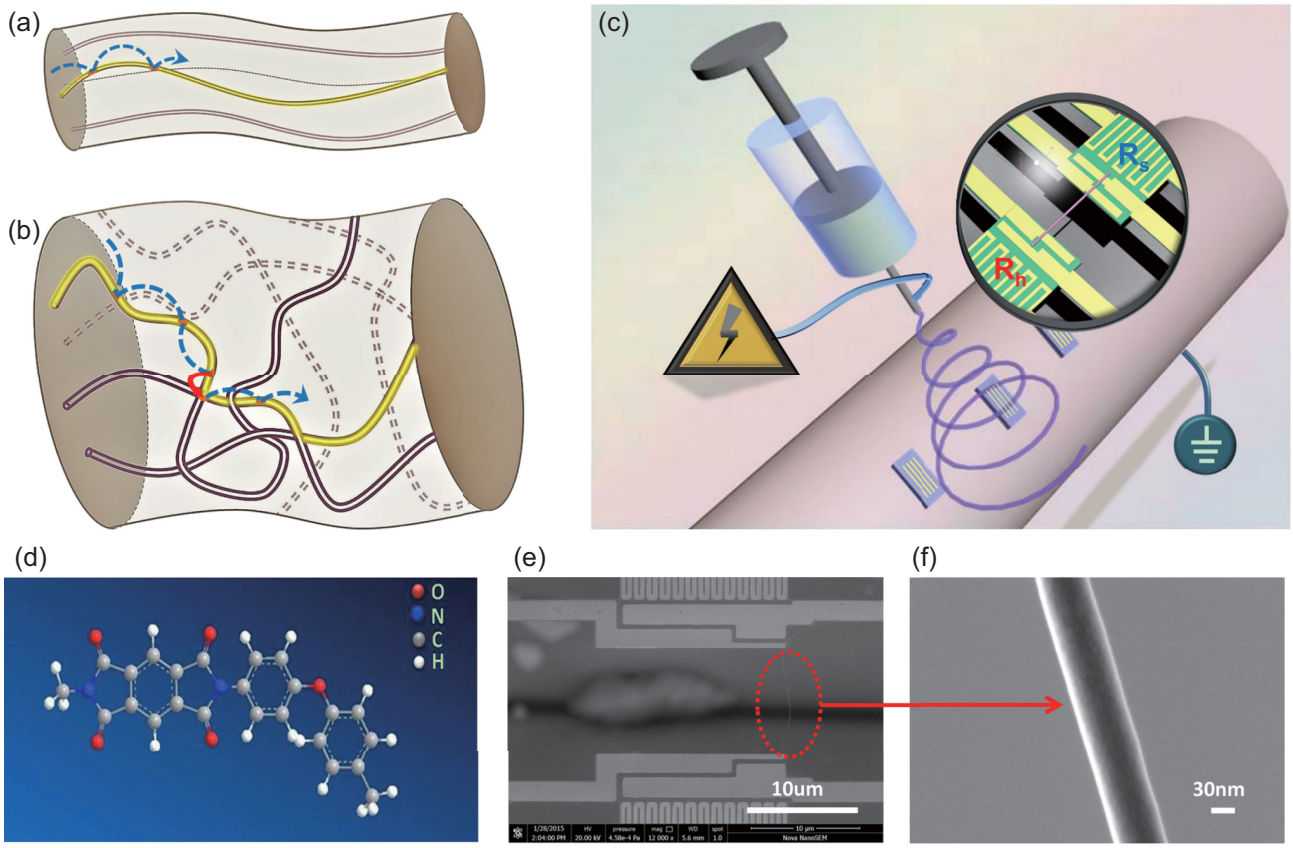

Figure 1. Schematic picture of the electrospinning setup and details of amorphous PI nanofibers. (a) Schematic of anisotropic quasi-1D thermal diffusion in nanofibers with small diameters. All the molecular chains are aligned along the fiber axis. The blue arrow denotes the hopping between neighboring localization centers within the chain and only intra-chain hopping could happen in this case. (b) Schematic of the quasi-isotropic thermal diffusion in nanofibers with large diameters. The molecular chains are randomly oriented and entangled with each other. Heat carriers hop equally to every direction and there is also the possibility of inter-chain hopping, denoted by the red arrow. (c) The electrospinning setup. Nanofiber was collected on the two suspended membranes (inset of Fig. 1c), which act as heater and temperature sensor during the thermal conductivity measurement. (d) 3D structural map of PI. (e) SEM image of PI nanofiber. The scale bar is 10 μm. The red circle marks the position of a single PI nanofiber. (f) Enlarged SEM image of the PI nanofiber shown in (e). The scale bar is 30 nm.

have been borrowed to qualitatively explain the thermal conductivity of amorphous polymers [4,27,28]. Compared to the unique type of hopping in inorganic amorphous materials, there are two types of hopping processes in bulk polymers, i.e., intra-chain and inter-chain hopping processes, which together with their interplay play an important role in the heat conduction. Therefore, the mechanism of the enhancement of thermal conductivity in polymer nanofibers and the upper limit of such enhancement when the polymer is stretched are not yet totally clear.

RESULTS AND DISCUSSION

Thanks to the development of experimental techniques, it is possible to characterize the thermal conductivity of ultra-thin polymer nanofibers. To test the microstructure dependence of thermal conductivity, it is straightforward to look into the diameter dependence of thermal conductivity in nanofibers through spinning or ultra-drawing [7,8], during which processes the entanglement of chains could be much reduced by adjusting controllable parameters such as the static-electrical field and draw ratio [29,30]. In this paper, we systematically investigate the microstructure dependence of thermal conductivity in polyimide (PI) nanofibers for different diameters. The diameters of the obtained PI nanofibers range from 31 nm to 167 nm (see Table S1) and the lengths of the obtained PI nanofibers are illustrated in Table S2. Molecular chains in thin nanofibers tend to align along the fiber axis with less entanglement, as Fig. 1a demonstrates, while chains in thicker nanofibers are randomly oriented and entangled with each other, as is illustrated in Fig. 1b.

Figure 1c presents a schematic diagram of the electrospinning setup. Due to the static-electrical

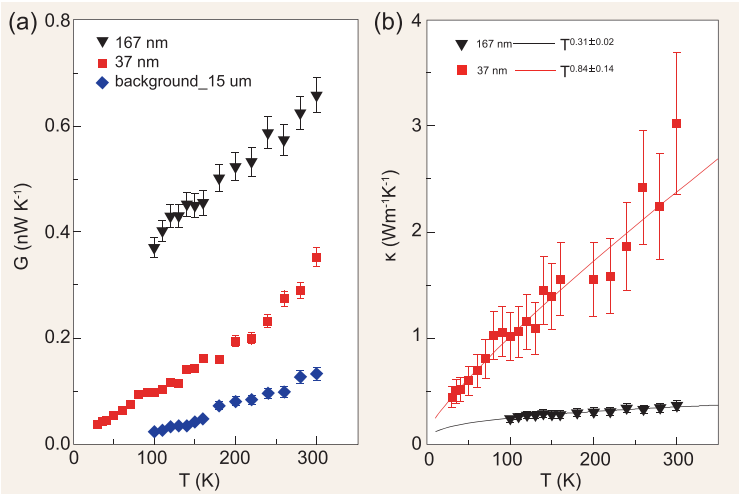

Figure 2. Thermal transport of PI nanofibers with different diameters as a function of temperature. (a) Thermal conductance of PI nanofibers. The blue rhombus points exhibit the thermal radiation measured by the differential circuit configuration with high vacuum (on the order of 1×10^{-8} mbar). (b) Thermal conductivity of PI nanofibers excluding thermal radiation for two samples: No. II $d = 37$ nm, $L = 14.8$ um; No. IX $d = 167$ nm, $L = 15.2$ um, respectively (the morphology details of other samples are illustrated in Tables S1 and S2 in the online supplementary data). Solid lines are fitted by $\kappa \sim T^{\lambda}$ with $\lambda = 0.84 \pm 0.14$ and 0.31 ± 0.02 for samples with diameters $d = 37$ nm and 167 nm, respectively. Error bars are estimated based on uncertainties associated with the fiber diameter and temperature uncertainty (see Tables S1 and S3 in the section entitled 'Thermal conductivity uncertainty' in the online supplementary data).

force introduced by high electrical voltage, suspended PI nanofibers were formed across two SiN_x membranes. These two SiN_x membranes were covered by platinum (i.e., the electrical ground). This was the key step where molecular chains tend to align along the axis of the nanofiber. There might be several PI nanofibers passing through the gap in the middle of the device after electrospinning. In our experiments, only one nanofiber is left; the others will be cut by a nanomanipulator with a tungsten needle (see Fig. S1). Figure 1d depicts a 3D structural map of PI. It shows large conjugated aromatic bonds in a PI structure, which could help to enhance the thermal conductivity of PI nanofibers [31].

Thermal conductivity along the fiber axis was measured by the traditional thermal bridge method [32–34] (Fig. 1e and f). The whole device was placed in a cryostat with high vacuum on the order of 1×10^{-8} mbar to reduce the thermal convection. To increase the measurement sensitivity, the differential circuit configuration (see Fig. S2a in the section entitled 'The differential circuit configuration' in the online supplementary data) was used and the measurement sensitivity of the thermal conductance increased from ~1 nW/K to 10 pW/K (see Fig. S2b in the section entitled 'The differential circuit configuration' in the online supplementary data) [33,35]. In our experiment, the thermal conductance of PI nanofibers with different diameters is on the order of 1×10^{-10} W/K (Fig. 2a). To eliminate the effect of thermal radiation, a blank suspended device was used to probe standard thermal radiation in a wide temperature range. The measured thermal radiation between the two suspended membranes in the blank device is around ~100 pW/K at room temperature. This result is a few times lower than that observed by Pettes *et al.* [36], probably due to the better vacuum level, which would reduce the air conduction and convection. In order to illustrate the effects of thermal contact resistance, two approaches were used to simulate the temperature distribution of the suspended membranes and calculate the thermal contact resistance at the platinum/PI nanofiber interface. These two approaches verified that the thermal contact resistance held a negligible contribution of the total measured thermal resistance (see Figs S3 and S4 and Table S4 in the sections entitled 'Finite element simulations (COMSOL Multiphysics 5.2)' and 'Thermal contact resistance' in the online supplementary data).

The measured thermal conductivity increases monotonously with temperature T, which is a typical feature of amorphous material, as Fig. 2b shows. The amorphous character of PI may arise from the defects and random bond angles within the chain, as well as the complex entanglement between chains. Furthermore, we find that the thermal conductivity varies with temperature as $\kappa \sim T^{\lambda}$, where λ varies from 0.31 ± 0.02 to 0.84 ± 0.14 as the diameter changes. For a thick nanofiber with diameter $d =$ 167 nm, the power law dependence $T^{0.31}$ agrees with the experimental measurement from Singh's group [4]. As the diameter decreases, the power index approaches 1, which coincides with the prediction of the hopping mechanism [24–26].

To look inside into the intrinsic dominant mechanism of thermal transport, the diameter dependence of thermal conductivity at room temperature is systematically investigated and the results are shown in Fig. 3. The thermal conductivity of PI nanofibers is close to that of bulk PI when the diameters are larger than 150 nm. It increases dramatically as the diameter decreases, and reaches an order of magnitude larger than that in bulk PI when the diameters are smaller than 40 nm. A similar result was also observed in electrospun nylon-11 nanofibers [12], which suggests that the stretching process could induce more ordered molecular chains in polymers, confirmed by high-resolution wide-angle X-ray scattering.

To describe the diameter dependence of the thermal conductivity quantitatively, we propose a theoretical model based on random walk theory to incorporate the diffusion of phonons through the

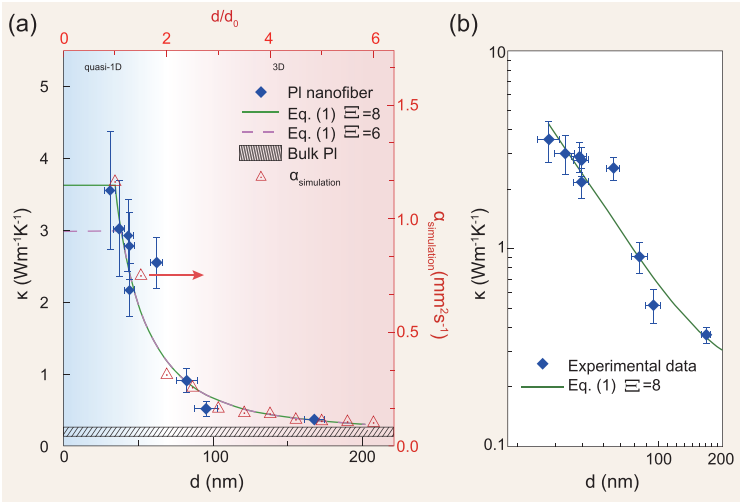

Figure 3. Dimensional crossover of thermal conductivity of PI nanofibers at room temperature. (a) The diameter and length details of PI nanofibers are illustrated in Tables S1 and S2 in the online supplementary data. The gray shadowed bar represents the thermal conductivity of bulk PI within the range of 0.1–0.3 Wm^{-1} K^{-1}. The rhombus (left axis and bottom axis) represents the experimental data. The olive solid line (left axis and bottom axis) and pink dashed line (left axis and bottom axis) are fitted by Equation (1) with different values of the parameter Ξ. Red triangles (right axis and upper axis) denote thermal diffusivity obtained from the random walk simulation (details of the random walk simulation are included in Fig. S5 and Table S5 in the section entitled 'Schematic of the diameter confinement effect on the coordination number' in the online supplementary data). (b) Dual-logarithm thermal conductivity versus diameter. The olive line is fitted by Equation (1).

hopping mechanism. We are aware that the lattice vibrations in disordered systems without periodicity do not have dispersion but the terminology of a 'phonon' is still usable to describe energy quanta. Considering a complex network with a large number of entangled macromolecular chains, phonons transport across this complex network through the hopping process. Note that there are two different types of hopping: intra-chain hopping, in which a phonon hops between localization centers within a single chain, as shown in Fig. 1a, and inter-chain hopping, in which a phonon hops from one chain to another chain, as shown in Fig. 1b. According to the random walk theory, the thermal diffusivity along the fiber axis is defined as [37] $\alpha = \frac{1}{\bar{Z}}\Gamma_{tot}\bar{R}^2$, where $\bar{Z}$ is the average effective coordination number along the fiber axis, $\bar{R}$ is the average hopping distance and Γ_{tot} is the temperature-dependent total hopping rate. In our simplified model, we do not consider the difference between the hopping rates of the inter- and intra-chain hopping processes. Note that the inter-chain hopping process usually happens at cross links of chains, in which case the hopping distance is negligible compared to that of the intra-chain hopping process; it is reasonable to assume that $\bar{R}$ is mainly determined by the intra-chain hopping distance R_{intra}.

Table 1. Fitting parameters obtained by fitting the experimental data in Fig. 3a with Equation (1).

Ξ	$\kappa_{quasi-1D}$ (Wm^{-1} K^{-1})	d_0 (nm)	Λ (nm)
6	3.0 ± 1.6	39 ± 13	62 ± 31
8	3.6 ± 2.2	34 ± 12	66 ± 36

The diameter dependence of $\bar{Z}$ is described by an empirical function $\bar{Z} = [2f(d)+1][\Xi f(d)+2]$, where $f(d) = 1 - 2/\{1+\exp[(d-d_0)/\Lambda]\}$ for $d > d_0$. In the above expression, d_0 is the critical diameter under which the diffusion converges to quasi-1D, Λ is the changing rate of the transition from quasi-1D to 3D and Ξ denotes the average number of inter-chain hopping sites. The average nearest inter-chain neighbor Ξ should be determined from the real configuration of polymer chains. From complex network theory, the number of nearest inter-chain neighbors should be 6–10 [38]. For further validation, numerical simulations in generating polymer chains are required. The current form of $f(d)$ could successfully describe the transition from 3D to quasi-1D. When $d = d_0$, $f(d) = 0$, meaning that the system is quasi-1D and there is no inter-chain hopping. When d approaches infinity, $f(d)$ saturates to 1, corresponding to the 3D system. We should stress that our empirical function is definitely not unique but it is one of the best ones (as is always the case in inverse problems) that fits the experimental data optimally. The thermal conductivity is expressed by $\kappa = \alpha\rho C_p$, where α is thermal diffusivity, ρ is mass density and C_p is specific heat capacity [39], thus thermal conductivity is inversely proportional to $\bar{Z}$ (details are given in the section entitled 'Diameter dependence of average coordination number' in the online supplementary data):

$$\kappa(d) = \frac{2\kappa_{quasi-1D}}{\bar{Z}}. \quad (1)$$

Note that $f(d) = 0$ when $d \le d_0$, and the thermal conductivity converges to $\kappa_{quasi-1D}$. This means that the thermal conductivity could not increase infinitely with decreasing fiber diameter. There exists an upper limit for the thermal conductivity of electrospun PI, corresponding to the 1D intra-chain diffusion, where the average effective coordination number along the fiber axis is 2. In this limit, all polymer chains are well aligned and the inter-chain interactions are negligible. To verify the validity of our model, we fit the experimental results with Equation (1). The fitting parameters are listed in Table 1. Our model fits well with the experimental data, as the lines in Fig. 3a show.

We also do a random walk simulation and obtain the dimensionless thermal diffusivity. The details of the simulation are included in the section entitled 'Random walk simulation' in the online supplementary data. The exact value of the thermal diffusivity of bulk PI is $\alpha_{\rm bulk} = 0.0775\ {\rm mm^2\,s^{-1}}$, estimated from the observed thermal conductivity of bulk PI $\kappa_{\rm PI} = 0.12\ {\rm Wm^{-1}\,K^{-1}}$, density of bulk PI $\rho_{\rm PI} = 1.42 \times 10^3\ {\rm kg\,m^{-3}}$, and specific heat of bulk PI $C_{p\rm PI} = 1.09 \times 10^3\ {\rm J\,kg^{-1}\,K^{-1}}$ [40]. Nanofibers with diameters smaller than d_0 exhibit quasi-1D thermal transport behavior, while nanofibers with diameters much larger than $d_0 + \Lambda$ tend to behave like bulk polymers. A crossover of heat conduction from quasi-1D to 3D is only apparent in the range $d_0 \leq d \lesssim d_0 + \Lambda$. The magnitude of critical diameter d_0 and parameter Λ is related to the radius of gyration $R_{\rm g}$ of macromolecular chains, which is typically on the order of tenths of nanometers [41]. $R_{\rm g}$ is determined by the structure of monomers, the bond angle between monomers, the length of a single chain, and the process condition such as applied voltage in electrospinning. When $d > d_0 + \Lambda \geq 2R_{\rm g}$, bulk-like polymer nanofibers can be realized since macromolecular chains can easily gyrate. When $d < d_0$, macromolecular chains can hardly gyrate and the chains prefer to lie along the fiber axis.

CONCLUSIONS

A crossover of heat conduction from 3D to quasi-1D has been observed experimentally in amorphous polymer nanofibers obtained from electrospinning. This behavior has been quantitatively explained by a model based on random walk theory in which both inter-chain and intra-chain hopping processes are considered. Two important fitting parameters, i.e., d_0 and Λ, are obtained as the characterization length of the dimensional transition. Our theory successfully testifies that the hopping mechanism based on the random walk picture is valid and it is useful to explain the diameter dependence of thermal conductivity in nanofibers. Nevertheless, there are still many open questions deserving further investigation. First, the temperature dependence of thermal conductivity has not been well explained and it requires deeper and quantitative understanding of the inter-chain thermal transport mechanism. Second, the four parameters in the empirical function require validation from further simulations and experiments. For example, $\kappa_{\rm quasi-1D}$ is closely related to the thermal conductivity of a single chain, and it can be obtained from molecular dynamics; Ξ, d_0 and Λ are determined by the configuration of polymer chains, which requires research on polymer condensed matter physics and thermal measurements on much thinner polymer fibers.

EXPERIMENTAL SECTION

Thermal conductivity measurement

The PI nanofibers fabricated by the electrospinning method served as bridge to connect two platinum/SiN_x membranes (Fig. 1e). These two membranes were regarded as thermometers. A DC current of a slow change step combined with an AC current (1000 nA) was added to one of the membranes serving as a heater resistor ($R_{\rm h}$, the left platinum coil shown in Fig. 1c). The DC current was applied to provide Joule heat and also to increase its temperature ($T_{\rm h}$). The AC current was used to measure the resistance of $R_{\rm h}$. Meanwhile, an AC current of the same value was applied to another membrane serving as sensor resistor ($R_{\rm s}$, the right platinum coil shown in Fig. 1c), to probe the resistance of $R_{\rm s}$. The Joule heating in $R_{\rm h}$ gradually dissipated through the six platinum/SiN_x beams and the PI nanofiber, which raises the temperature in $R_{\rm s}$ ($T_{\rm s}$). At steady state, the thermal conductance of the PI nanofibers ($\sigma_{\rm PI}$) and the thermal conductance of the suspended beam ($\sigma_{\rm l}$) could be obtained by

$$\sigma_{\rm l} = \frac{Q}{\Delta T_{\rm h} + \Delta T_{\rm s}}$$

and

$$\sigma_{\rm PI} = \frac{\sigma_{\rm l}\Delta T_{\rm s}}{\Delta T_{\rm h} - \Delta T_{\rm s}},$$

where $\Delta T_{\rm h}$ and $\Delta T_{\rm s}$ indicate the temperature rise in $R_{\rm h}$ and $R_{\rm s}$, and Q is the Joule heat applied to the heater resistor and one of the platinum/SiN_x beams.

Electrospinning

To fabricate nanoscale PI fibers with controllable diameters and chain orientations, we utilized electrospinning using a commercialized electrospinner. The solvent, a mixture of PI and dimethylformamide (DMF) solution, was prepared with concentrations from 45% to 80%, followed by all-night stirring to guarantee complete mixing of the PI molecules and DMF solvent. The diameter of the PI nanofiber should increase with increasing PI molecule weight ratio.

SUPPLEMENTARY DATA

Supplementary data are available at *NSR* online.

ACKNOWLEDGEMENTS

Special thanks go to the technical engineer Ning Liu from ZEISS, who helped to obtain the high-resolution SEM image. In addition, Lan Dong wants to thank the support and company from Tongren Liu in the last few years when pursuing her Ph.D degree in Tongji University.

FUNDING

This work was supported by the National Natural Science Foundation of China (11674245, 11334007 and 11505128), the program for Professor of Special Appointment (Eastern Scholar) at Shanghai Institutions of Higher Learning (TP2014012), the Shanghai Committee of Science and Technology in China (17142202100 and 17ZR1447900), and the Fundamental Research Funds for Central Universities.

Conflict of interest statement. None declared.

REFERENCES

1. Wang XJ, Ho V and Segalman RA *et al.* Thermal conductivity of high-modulus polymer fibers. *Macromolecules* 2013; **46**: 4937–43.
2. Springer LH. *Introduction to Physical Polymer Science*. Hoboken: Wiley-Interscience, 2006.
3. Kim GH, Lee D and Shanker A *et al.* High thermal conductivity in amorphous polymer blends by engineered interchain interactions. *Nat Mater* 2015; **14**: 295–300.
4. Singh V, Bougher TL and Weathers A *et al.* High thermal conductivity of chain-oriented amorphous polythiophene. *Nat Nanotech* 2014; **9**: 384–90.
5. Moore AL and Shi L. Emerging challenges and materials for thermal management of electronics. *Mater Today* 2014; **17**: 163–74.
6. Waldrop MM. More than Moore. *Nature* 2016; **530**: 144–7.
7. Choy CL. Thermal conductivity of polymers. *Polymer* 1977; **18**: 984–1004.
8. Choy CL, Luk WH and Chen FC. Thermal conductivity of highly oriented polyethylene. *Polymer* 1978; **19**: 155–62.
9. Choy CL, Wong YW and Yang GW *et al.* Elastic modulus and thermal conductivity of ultradrawn polyethylene. *J Polymer Sci B Polymer Phys* 1999; **37**: 3359–67.
10. Shen S, Henry A and Tong J *et al.* Polyethylene nanofibres with very high thermal conductivities. *Nat Nanotech* 2010; **5**: 251–5.
11. Ma J, Zhang Q and Mayo A *et al.* Thermal conductivity of electrospun polyethylene nanofibers. *Nanoscale* 2015; **7**: 16899–908.
12. Zhong Z, Wingert MC and Strzalka J *et al.* Structure-induced enhancement of thermal conductivities in electrospun polymer nanofibers. *Nanoscale* 2014; **6**: 8283–91.
13. Cao B-Y, Li Y-W and Kong J *et al.* High thermal conductivity of polyethylene nanowire arrays fabricated by an improved nanoporous template wetting technique. *Polymer* 2011; **52**: 1711–5.
14. Cao B-Y, Kong J and Xu Y *et al.* Polymer nanowire arrays with high thermal conductivity and superhydrophobicity fabricated by a nano-molding technique. *Heat Trans Eng* 2013; **34**: 131–9.
15. Liu J and Yang R. Tuning the thermal conductivity of polymers with mechanical strains. *Phys Rev B* 2010; **81**: 174122.
16. Zhang T, Wu XF and Luo TF. Polymer nanofibers with outstanding thermal conductivity and thermal stability: fundamental linkage between molecular characteristics and macroscopic thermal properties. *J Phys Chem C* 2014; **118**: 21148–59.
17. Zhang T and Luo TF. Role of chain morphology and stiffness in thermal conductivity of amorphous polymers. *J Phys Chem B* 2016; **120**: 803–12.
18. Wei XF, Zhang T and Luo TF. Chain conformation-dependent thermal conductivity of amorphous polymer blends: the impact of inter- and intra-chain interactions. *Phys Chem Chem Phys* 2016; **18**: 32146–54.
19. Allen P and Feldman J. Thermal conductivity of disordered harmonic solids. *Phys Rev B* 1993; **48**: 12581–8.
20. Feldman J, Kluge M and Allen P *et al.* Thermal conductivity and localization in glasses: numerical study of a model of amorphous silicon. *Phys Rev B* 1993; **48**: 12589–602.
21. Einstein A. Elementare Betrachtungen über die thermische Molekularbewegung in festen Körpern. *Ann Phys* 1911; **340**: 679–94.
22. Cahill DG, Watson SK and Pohl RO. Lower limit to the thermal conductivity of disordered crystals. *Phys Rev B* 1992; **46**: 6131–40.
23. Hsieh WP, Losego MD and Braun PV *et al.* Testing the minimum thermal conductivity model for amorphous polymers using high pressure. *Phys Rev B* 2011; **83**: 174205.
24. Alexander S, Entin-Wohlman O and Orbach R. Phonon-fracton anharmonic interactions: the thermal conductivity of amorphous materials. *Phys Rev B* 1986; **34**: 2726–34.
25. Nakayama T and Orbach R. Anharmonicity and thermal transport in network glasses. *Europhys Lett* 1999; **47**: 468–73.
26. Takabatake T, Suekuni K and Nakayama T *et al.* Phonon-glass electron-crystal thermoelectric clathrates: experiments and theory. *Rev Mod Phys* 2014; **86**: 669–716.
27. Keblinski P, Shenogin S and McGaughey A *et al.* Predicting the thermal conductivity of inorganic and polymeric glasses: the role of anharmonicity. *J Appl Phys* 2009; **105**: 034906.
28. Xie X, Yang KX and Li DY *et al.* High and low thermal conductivity of amorphous macromolecules. *Phys Rev B* 2017; **95**: 035406.
29. Arinstein A, Liu Y and Rafailovich M *et al.* Shifting of the melting point for semi-crystalline polymer nanofibers. *Europhys Lett* 2011; **93**: 46001.
30. Greenfeld I, Arinstein A and Fezzaa K *et al.* Polymer dynamics in semidilute solution during electrospinning: a simple model and experimental observations. *Phys Rev E* 2011; **84**: 041806.
31. Liu J and Yang RG. Length-dependent thermal conductivity of single extended polymer chains. *Phys Rev B* 2012; **86**: 104307.
32. Shi L, Li D and Yu C *et al.* Measuring thermal and thermoelectric properties of one-dimensional nanostructures using a microfabricated device. *J Heat Transfer* 2003; **125**: 881–8.
33. Liu D, Xie RG and Yang N *et al.* Profiling nanowire thermal resistance with a spatial resolution of nanometers. *Nano Lett* 2014; **14**: 806–12.

34. Xu XF, Pereira LF and Wang Y *et al*. Length-dependent thermal conductivity in suspended single-layer graphene. *Nat Commun* 2014; **5**: 3689.
35. Wingert MC, Chen ZC and Kwon S *et al*. Ultra-sensitive thermal conductance measurement of one-dimensional nanostructures enhanced by differential bridge. *Rev Sci Instrum* 2012; **83**: 024901.
36. Pettes MT, Jo I and Yao Z *et al*. Influence of polymeric residue on the thermal conductivity of suspended bilayer graphene. *Nano Lett* 2011; **11**: 1195–200.
37. Mehrer H. *Diffusion in Solids*. Berlin: Springer Science and Business Media, 2007.
38. Watts DJ and Strogatz SH. Collective dynamics of 'small-world' networks. *Nature* 1998; **393**: 440–2.
39. Haynes MW, Lide RD and Bruno JT. *CRC Handbook of Chemistry and Physics*. Boca Raton: CRC Press, 2014.
40. 6.777J/2.751J Material Property Database. http://www.mit.edu/~6.777/matprops/polyimide.htm. (4 April 2017, date last accessed).
41. Li B, He T and Ding M *et al*. Chain conformation of a high-performance polyimide in organic solution. *Polymer* 1998; **39**: 3193–7.